SUPPLEMENTAL MATERIAL

Ucar et al., https://doi.org/10.1084/jem.20170416

A Major cell population comparisons (%)

	Mean (HY)	Mean (HO)	SD (HY)	SD (HO)	Dif (HY-HO)	p-value (Wilcox)
CD14	15.7	15.6	7.4	5.4	0.1	0.993
CD19	7.5	5.4	3	3.4	2.1	0.014
CD4	30.7	28.5	7.8	10.4	2.2	0.526
CD8	15.6	10.5	4.7	7	5.1	0.006

B CD4+ T cell subset comparisons (%)

	Mean (HY)	Mean (HO)	SD (HY)	SD (HO)	Dif (HY-HO)	p-value (Wilcox)
Total	30.4	29.7	7.9	9.1	0.7	0.875
Naive	11.1	7.8	6.3	5.4	3.4	0.047
CM	7.9	7.6	4.1	4.4	0.3	0.559
EM	9.1	11.8	4.8	4.5	-2.7	0.024
EMRA	2.4	2.5	2.4	2.1	-0.1	0.610

C CD8+ T cell subset comparisons (%)

	Mean (HY)	Mean (HO)	SD (HY)	SD (HO)	Dif (HY-HO)	p-value (Wilcox)
Total	15.6	10.9	4.6	7.4	4.7	0.022
Naive	7.2	3.2	3.2	4.1	4	1.E-04
CM	1.1	1.2	0.9	1.3	-0.1	0.441
EM	3.5	2.6	3.7	1.9	0.9	0.162
EMRA	3.7	4	2.3	4.1	-0.3	0.630

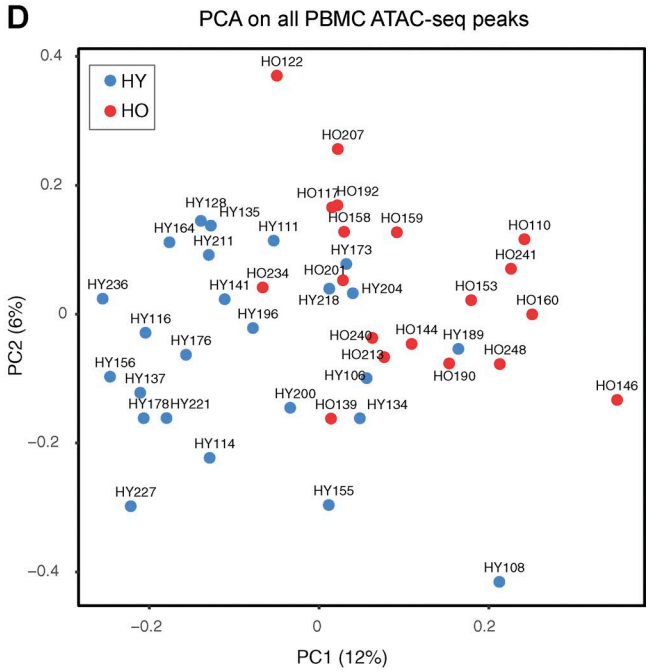

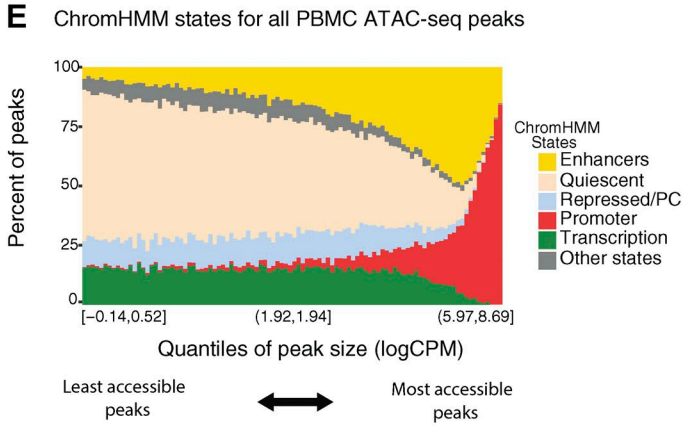

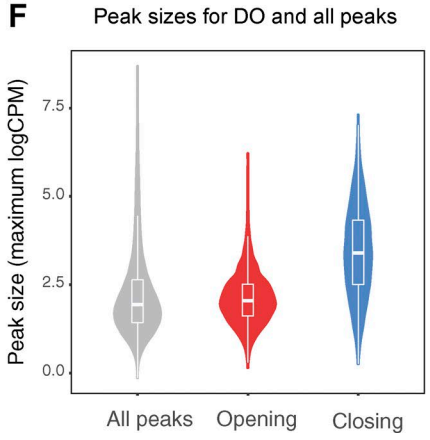

Figure S1. **Cell composition changes with aging.** (A) Changes in major cell compositions with aging. Note the significant decrease in total CD19$^+$ and CD8$^+$ T cells. (B) Changes in CD4$^+$ T cells subsets with aging. A significant increase in EM cells is observed. (C) Changes in CD8$^+$ T cells subsets with aging. A significant decrease in naive CD8$^+$ T cells is observed. P values for all comparisons were calculated using the Wilcoxon test. (D) Sample loadings on first and second principal components (PCs) computed based on adjusted reads estimated for all of the PBMC ATAC-seq peaks scored in this study (n = 140,172 peaks). Age groups tend to cluster separately, implying aging as a leading factor explaining epigenetic variation in PBMCs. (E) Relationship between peak size (i.e., normalized read counts within peak) and functional annotations, as annotated using Roadmap chromHMM states for PBMCs. Larger, more accessible peaks are more likely to be found at promoters (red bars) and enhancers (yellow), whereas small peaks are more likely to be called at inactive regions, represented by quiescent (salmon) and repressed sites (slate). (F) Distribution of peak sizes (maximum logCPM of read counts among all samples) as a function of aging-related changes in peak accessibility for all, differentially closing, and differentially opening peaks.

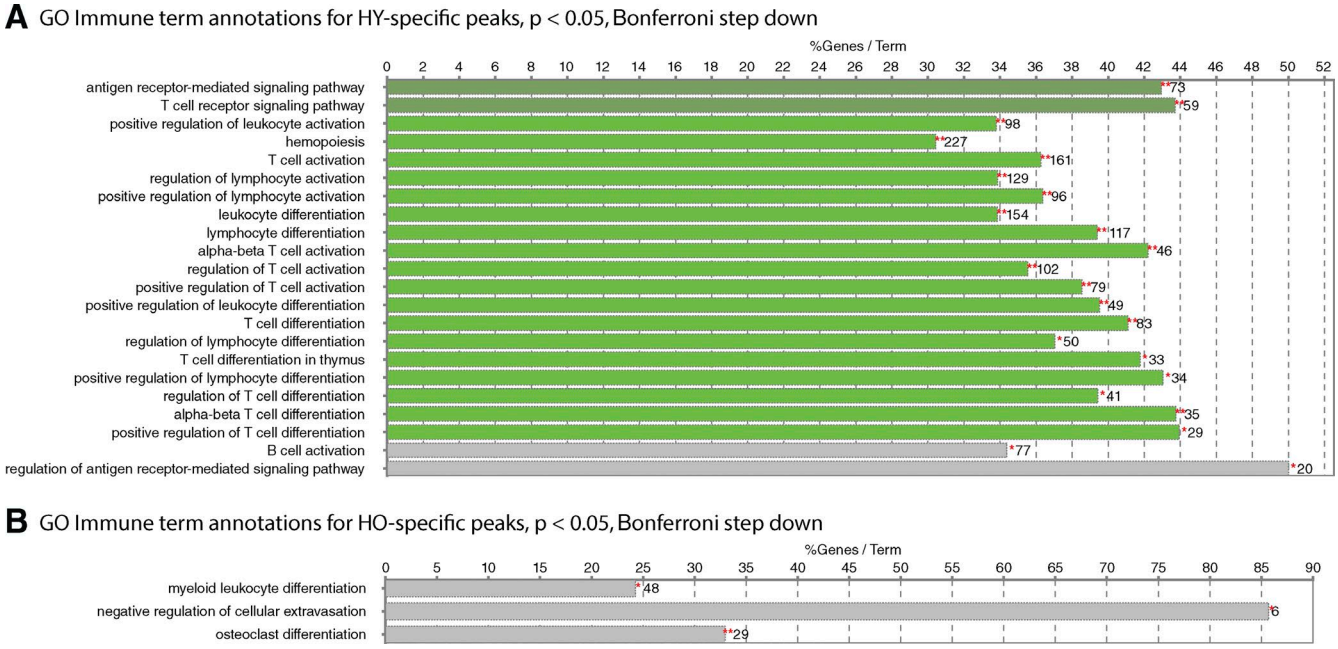

Figure S2. **Immune genes are affected by chromatin remodeling.** (A) ClueGO GO term enrichment results for HY-specific peaks, evaluated at a P value of less than 0.05 after Bonferroni step-down correction. Bars are proportional to the percentage of genes in each enriched GO term that is also present in the query set, whereas numbers next to the bars indicate the corresponding gene count. (B) ClueGO enrichment results for HO-specific peaks, evaluated at a P value of less than 0.05 (no correction). Bars and numbers next to them represent, respectively, the percentage and total number of genes in each enriched GO term and also present in the query set.

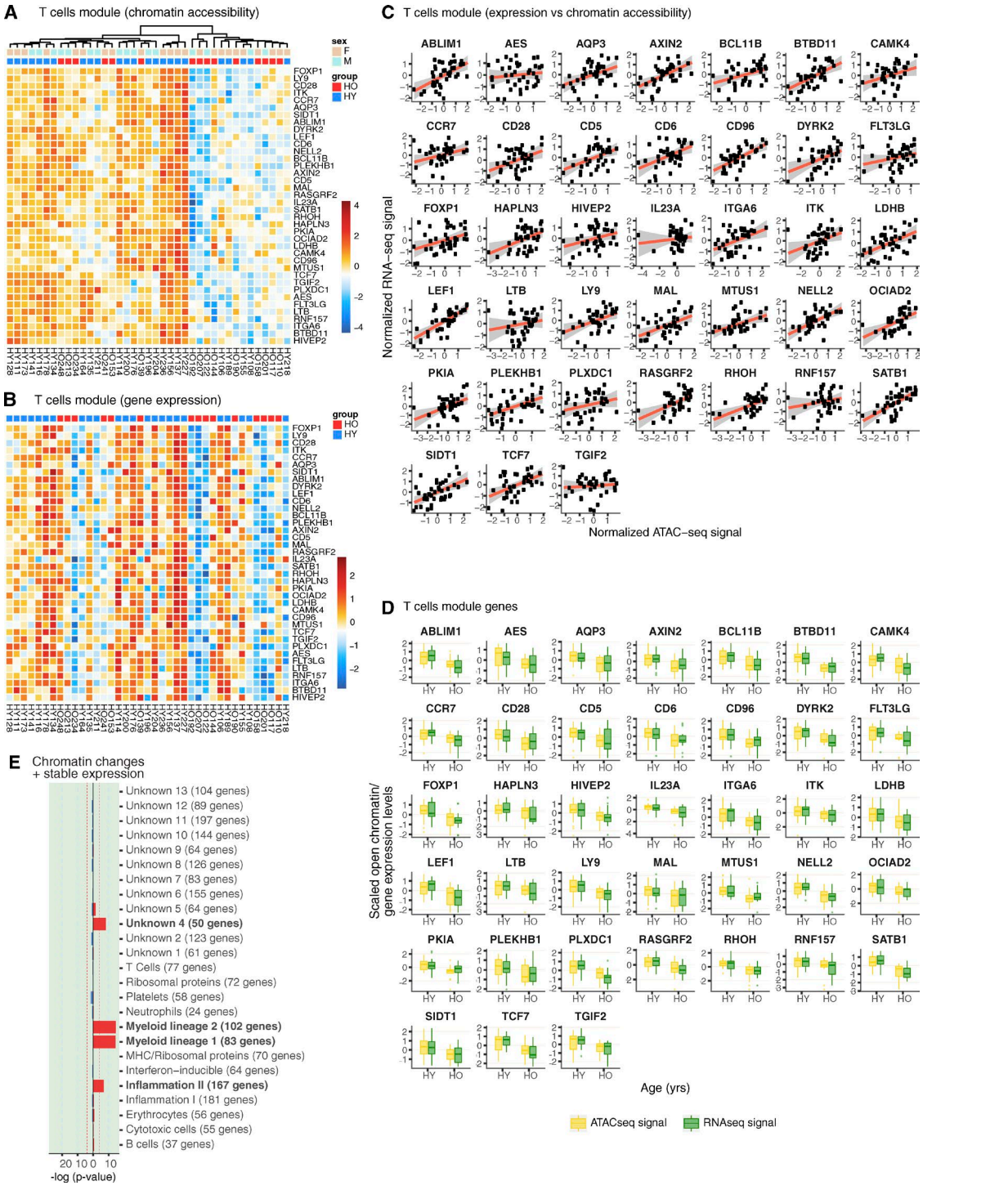

Figure S3. **The T cell module is epigenetically and transcriptionally repressed with aging.** (A) Personal profiles of chromatin accessibility of promoter peaks associated to genes in the T cell module for which both chromatin accessibility and gene expression decrease with aging. (B) Personal profiles of gene expression of genes in the T cell module, with samples and genes sorted to match the clustering computed based on chromatin accessibility. (C) Plot of gene expression versus chromatin accessibility for subject-matched samples for genes with aging-related promoter closing and lost expression in the T cell module. (D) Plot of chromatin accessibility (in yellow) and expression (in green) by age group for matched samples for genes in the T cell module with aging-related decreases in accessibility and expression. (E) Immune module enrichment of genes that undergo loss of accessibility with aging but that are transcriptionally stable. Plot shows -log10 of P values from a hypergeometric test; reference lines are drawn at the largest P value for which a 5% FDR is attained.

A Top 15 peaks associated with chromatin closing

Gene Name	# of closing peaks	Average FDR	Average logFC	Average logCPM
ETS1	24	2.05E-02	-0.40	2.17
TGFBR2	15	8.75E-03	-0.49	2.40
FAM65B	13	5.95E-03	-0.48	2.21
BACH2	13	8.00E-03	-0.51	2.32
FOXP1	12	1.05E-02	-0.46	2.57
IL7R	12	4.89E-03	-0.60	2.12
BRINP3	11	3.03E-02	-0.41	0.92
CCR7	11	9.36E-03	-0.53	2.45
NCK2	11	9.11E-03	-0.43	2.81
CDC42SE2	11	1.15E-02	-0.38	2.75
LRRN3	11	5.26E-03	-0.58	1.96
IKZF1	11	1.25E-02	-0.44	2.86
PTPRC	10	2.05E-02	-0.35	2.88
CD44	10	1.03E-02	-0.47	2.56
SNX9	10	1.43E-02	-0.43	2.57

B Top 15 peaks associated with chromatin opening

Gene Name	# of closing peaks	Average FDR	Average logFC	Average logCPM
MAF	18	1.71E-02	0.42	1.25
FGFR2	9	1.64E-02	0.51	0.67
ELK2AP	9	1.63E-02	0.51	2.17
CPZ	9	2.11E-02	0.51	1.01
ZNF618	8	2.61E-02	0.40	1.24
KIF26A	7	2.49E-02	0.42	1.40
EGLN3	7	1.97E-02	0.44	0.85
APBA2	7	9.34E-03	0.43	1.71
NPIPA7	7	1.37E-02	0.59	0.77
VAC14	7	2.82E-02	0.34	2.09
ZNF469	7	1.61E-02	0.49	1.27
AGAP1-IT1	7	1.76E-02	0.44	0.88
CDH4	7	2.61E-02	0.45	1.22
DAB2IP	7	2.36E-02	0.42	1.30
ARHGEF10L	6	2.69E-02	0.39	1.22

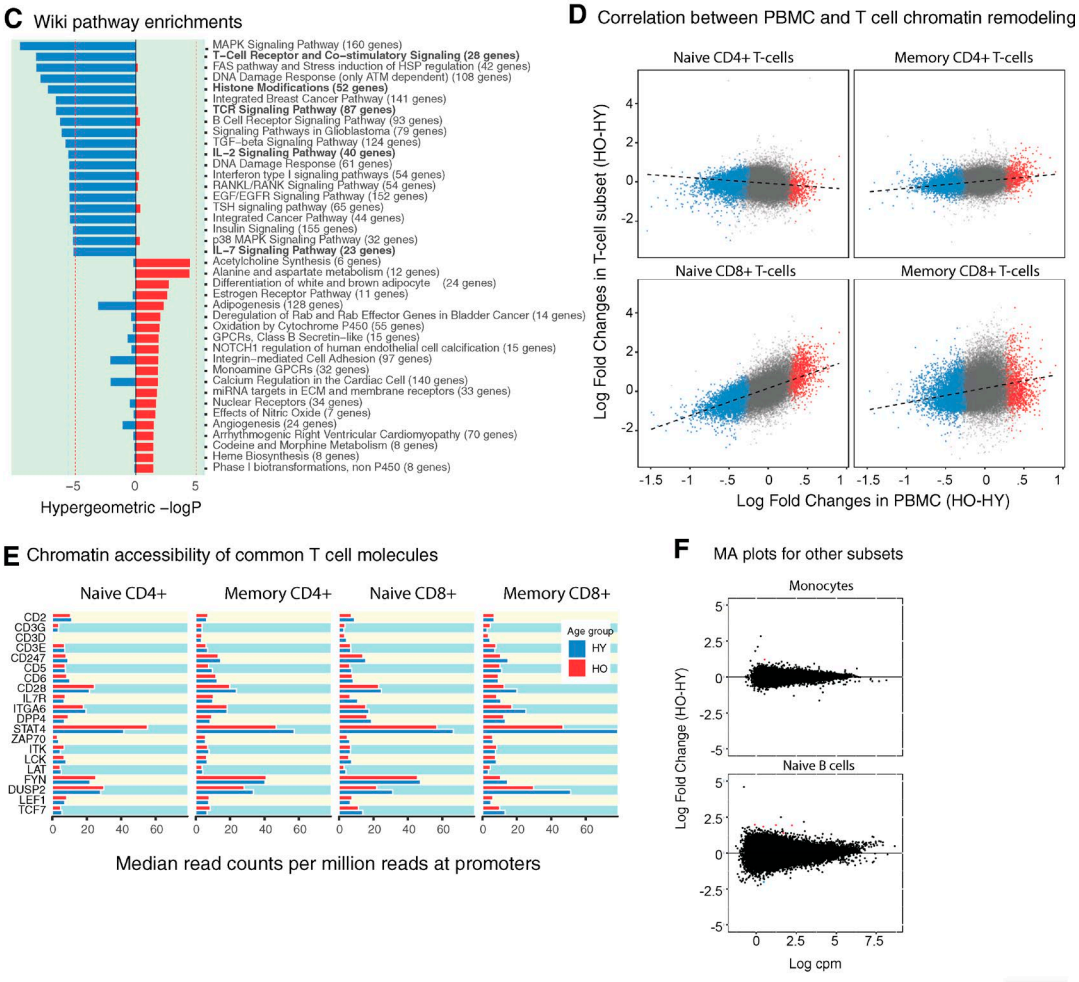

Figure S4. **T cell signaling pathways in CD8⁺ T cells are impaired with aging.** (A) Top 15 genes associated with chromatin closing with aging. Genes are sorted with respect to the number of significantly closing peaks annotated to their promoters. *IL7R* is a top gene in this list, with 12 closing peaks. (B) Top 15 genes associated with chromatin opening with aging. Genes are sorted with respect to the number of significantly opening peaks annotated to their promoters. (C) WikiPathways enrichment results for genes associated with closing (blue bars) and opening (red bars) peaks. P values computed using hypergeometric tests. Reference lines are drawn at the largest P value for which a 5% FDR is attained, determined using the Benjamini-Hochberg method. (D) Correlation between chromatin remodeling in PBMCs and chromatin remodeling in T cell subsets. Pearson correlation values indicate that PBMCs correlate differently with different T cells, where this correlation is higher for CD8⁺ T cells than for CD4⁺ T cells. (E) Median chromatin accessibility at the promoters of selected functionally relevant signaling and surface molecules in naive and memory CD4⁺ and CD8⁺ T cells. (F) Chromatin accessibility log2 fold change (old-young) versus mean read count for ATAC-seq peaks for monocytes (top) and naive B cells (bottom). Peaks differentially opening (closing) with aging are represented in red (blue; 5% FDR). Testing of differential chromatin accessibility based on a GLM applied to ATAC-seq peak read counts, with significance assessed at a 5% FDR threshold computed using Benjamini-Hochberg adjustment. There are nearly zero aging differential peaks in these cell types.

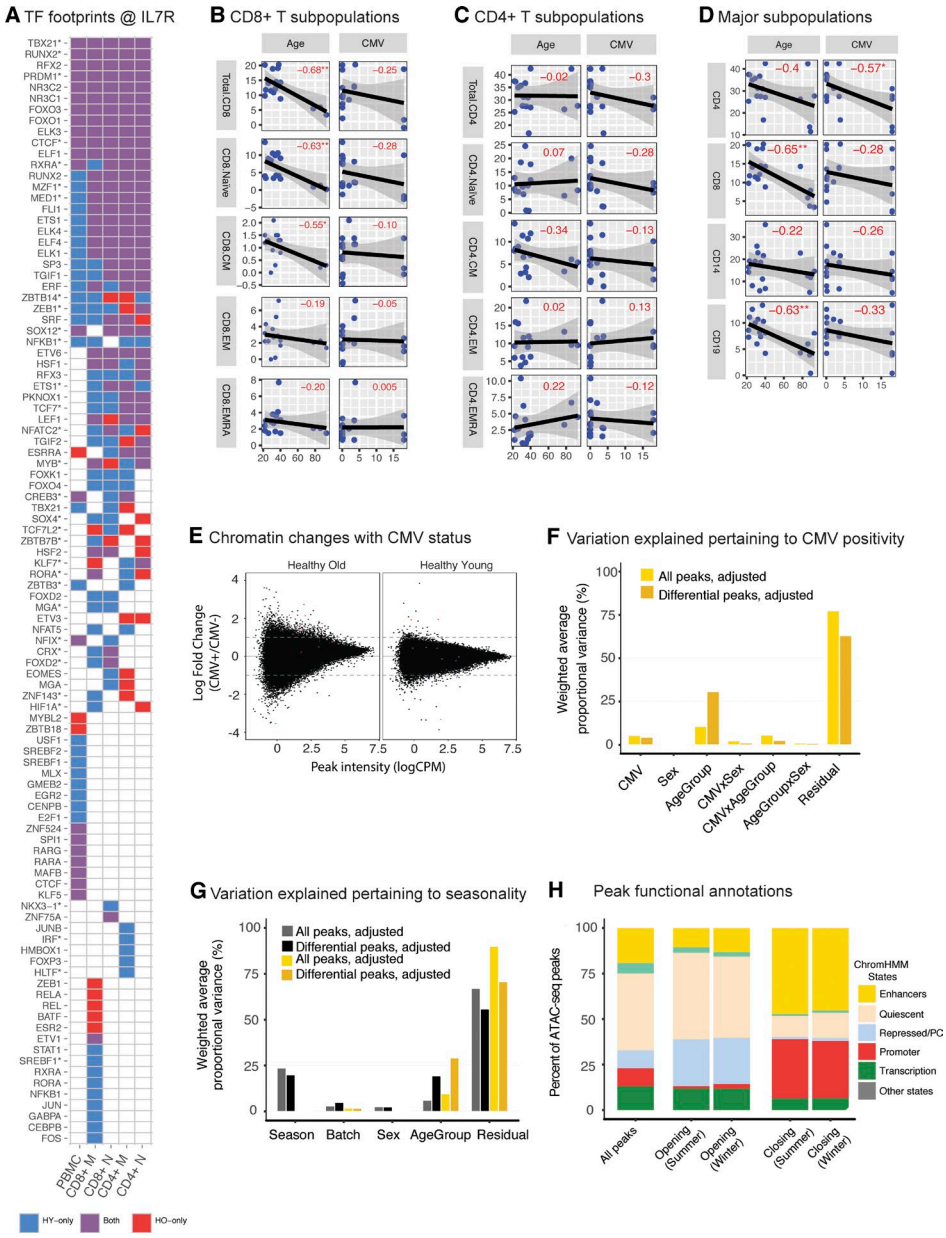

Figure S5. **CMV- and season-related chromatin changes in PBMCs.** (A) A heat map representing whether a TF footprint is called near the IL7R gene promoter in a given cell type. Red (blue) indicates that footprinting is found only in HO (HY) samples, whereas purple indicates that footprints for a TF motif are found in both HO and HY subjects. About half of the listed TFs have footprints in all cell types. (B) Correlation between $CD8^+$ T cell subset counts and age (left) and CMV antibody levels (right). The most significant effect occurs on naive $CD8^+$ T cells counts with aging. (C) Correlation between $CD4^+$ T cell subset counts and age (left) and CMV antibody levels (right). (D) Correlation between major immune cell subset counts and age (left) and CMV antibody levels (right). (E) Plot showing log2 fold change of chromatin accessibility relative to CMV status (i.e., CMV^+ vs. CMV^-) versus mean read count of ATAC-seq peaks when samples are stratified based on age groups. No significant chromatin remodeling associated with CMV status was observed within either age group. (F) Variation in PBMC chromatin accessibility (read counts at ATAC-seq peaks) explained by CMV and other factors, as quantified by PVCA for all peaks and peaks significantly remodeled with aging. Neither CMV nor the CMV × age interaction contributes much to the variance. Adjusted peak scores are obtained after fitting a GLM including CMV as a blocking factor. (G) Variation in PBMC chromatin accessibility explained by aging, seasonality, sex, library preparation batch, and other factors, as quantified by PVCA. Seasonality, unlike sex or batch, contributes significantly to the variation, prompting its inclusion as a covariate in our models. Adjusted peak scores were obtained after fitting a GLM including season as a blocking factor; normalized peaks lack this adjustment. (H) ChromHMM annotations of all and differentially open/closed peaks obtained from summer and winter samples. Similar distributions were observed for both seasons; this also resembles the global pattern of variation. All differential analyses of chromatin accessibility were performed using GLMs, with significance assessed at a 5% FDR after Benjamini-Hochberg adjustment. CMV–aging comparisons based on $n = 12$ young and $n = 9$ elderly subjects ($n = 11$ CMV^+, $n = 10$ CMV^-). Season–aging comparisons based on $n = 25$ young and $n = 19$ elderly subjects ($n = 17$ summer, $n = 27$ winter samples).

Tables S1–S10 are provided as Excel files.

Table S1. Cohort information: Detailed sample metadata, including samples used in ATAC-seq and RNA-seq analyses, as well as samples used as source of other types of data (cell composition, CMV status).

Table S2. Cell composition: Proportion values of sorted T cell and major cell populations ($CD4^+$, $CD8^+$, $CD14^+$, $CD19^+$) in PBMC extracts from subjects included in this study.

Table S3. Genes associated with differentially (A) closing and (B) opening ATAC-seq peaks.

Table S4. Enrichment of immune GO terms and WikiPathways pathways in differentially closing and opening ATAC-seq peaks. Results from ClueGO analysis.

Table S5. Enrichment of immune GO, biological process GO, WikiPathways pathways, and KEGG pathways in immune modules annotated as unknown in Figs. 2 C and 3 B.

Table S6. Fraction of $IL7R^+$ cells among $CD4^+$, $CD8^+$, $CD19^+$, and $CD14^+$ HY and HO samples, showing that a decrease in this fraction correlates to age only in $CD8^+$ compartment cells.

Table S7. TF motifs found near IL7R promoters. List built using MotifMap at a 20% FDR level.

Table S8. Genome-wide fraction of footprints called for each TF motif in HY and HO subjects in each T cell subset. Only footprints overlapping gene promoters are included in calculations. Proportion is computed over all footprint locations called in either or in both merged HY and HO samples. Footprints called separately in each cell subpopulation.

Table S9. Sample information used for determination of CMV status.

Table S10. ATAC-seq and RNA-seq data quality metrics for samples analyzed in this study.